Characterization of a flow-through microcalorimeter for measuring the heat production of cardiac trabeculae

A. J. Taberner and I. W. Hunter
Bioinstrumentation Laboratory, Department of Mechanical Engineering, Massachusetts Institute of Technology, 77 Massachusetts Avenue, Cambridge, Massachusetts 02139

R. S. Kirton, P. M. F. Nielsen, and D. S. Loiselle
Bioengineering Institute, The University of Auckland, Private Bag 92019, Auckland 1020, New Zealand

(Received 26 April 2005; accepted 22 August 2005; published online 11 October 2005)

The energy consumption of isolated cardiac trabeculae can be inferred from measurements of their heat production. Once excised from the heart, to remain viable, trabeculae require continuous superfusion with an oxygen- and nutrient-rich solution. Flow-through calorimeters enable trabeculae to be maintained in a stable and controlled environment for many hours at a time. In this paper we describe and characterize a flow-through microcalorimeter, with sensitivity in the 1 μW range, for measuring the heat output of 10 μg cardiac trabeculae. The device uses infrared-sensitive, thin-film thermopile sensors to provide a noncontact method for measuring temperature differences. The sensors are capable of resolving 5 μK temperature differences within the superfusing fluid. The microcalorimeter has a sensitivity of 2.56 V/W at a flow rate of 1 μl/s, with a time constant of approximately 3.5 s. The sensitivity and time constant are strongly dependent upon the flow rate. Predictions of a finite-element model of the calorimeter's characteristics compare favorably with measured data over a wide range of flow rates. © *2005 American Institute of Physics.*
[DOI: 10.1063/1.2093769]

I. INTRODUCTION

Cardiac muscle consumes energy as adenosine triphosphate (ATP) is hydrolyzed within its cells. ATP hydrolysis provides the Gibbs free energy for the maintenance of cellular integrity and for the performance of electrical, chemical (osmotic), and mechanical work. Since the energy-conversion processes are imperfect,[1] heat is produced within, and subsequently liberated by, the muscle. The measurement of muscle heat production (especially if coupled with the measurement of muscle mechanics) provides insight into the thermodynamics of the energy-consuming processes that occur within the muscle.

An appropriate method for inferring the heat output and, thereby, the energy consumption of the muscle is to measure the temperature increase imparted by the muscle to a flowing fluid. For a given flow rate, the heat liberated by the muscle causes a proportional increase in the temperature of the superfusate. Rat right-ventricular trabeculae ($\sim$2 mm long $\times$200 μm diameter) provide appropriate test specimens for such a technique, since their small diameter diminishes the possibility of oxygen deprivation within the muscle tissue.[2] However, owing to their small volume ($\sim 10^{-10}$ m^3), the heat liberated by cardiac trabeculae is meager ($\sim$10 μW), and the typical temperature increase they impart to a superfusing fluid (flowing at $\sim$1 μl/s) is only of the order of 1 mK[3]. Hence, a highly sensitive flow-through calorimeter is required for making heat measurements.

Previously constructed flow-through muscle calorimeters[3–5] have utilized thin-wire thermocouple arrays, yielding a modest sensitivity. Flow injection calorimeters,[6] microphysiometers,[7] and microbiosensors[8] commonly use custom thin-film thermopile sensors. These sensors consist of arrays of thermocouples (BiSb/Sb, Al/p^+-polysilicon, etc.) deposited on a thin ($<$1 μm) membrane of SiO_2–Si_3N_4. The fragile membrane (sometimes coated with silicone rubber for additional robustness) is usually brought into intimate contact with a stationary or flowing fluid.

We have designed and constructed a flow-through calorimeter that utilizes a novel noncontact arrangement of thin-film thermopile sensors to measure the temperature increase of an oxygen- and nutrient-rich superfusion solution as it flows over a cardiac trabecula. Our approach exploits the high sensitivity of commercially available thermopile sensors while avoiding the need for a fluid to come into contact with the thermopile membrane.

II. DESIGN

Our microcalorimeter comprises a measurement chamber consisting of a 7-mm-long borosilicate glass tube of square cross-section (1 mm inside width, 200 μm wall thickness) glued into a gold- and nickel-plated tellurium-copper housing (Fig. 1). The ends of the glass tube are unobstructed, allowing quartz tubes (700 μm o.d. 500 μm i.d.) to intrude from either end. A muscle-securing platinum hook (manufactured using the wire electro-discharge machining process) is glued into the tip of each quartz tube. An isonel-insulated platinum wire (25 μm diameter) is soldered to the back of each hook and threaded back through the quartz tubes to facilitate the electrical stimulation of the muscle and the Joule heating of the fluid between the hooks.

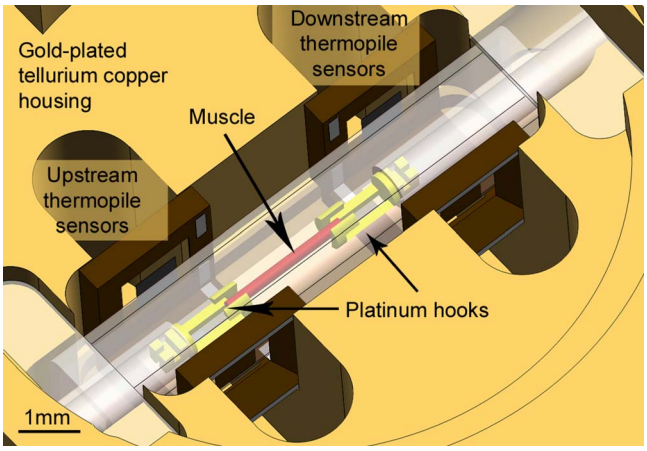

FIG. 1. (Color online) Closeup view of measurement chamber and sensors.

Oxygenated superfusate is passed through a heat exchanger, fed into the left-hand (upstream) end of the chamber past the specimen, and removed from the right-hand (downstream) end by a nonpulsatile vacuum fluid removal system. Surface tension prevents the fluid from spilling from the open, left-hand end of the chamber. Exudate from the right-hand end is collected in a computer-interfaced microbalance (Scout Pro, Ohaus Corporation, NJ, USA), and its flow rate computed over time from its cumulative weight.

Two thermopile arrays (each consisting of three thermopile sensors (TS10, HLPlanarTechnik GmBH, Dortmund, Germany)] measure the surface temperature of the measurement chamber, relative to that of the housing, upstream and downstream of the specimen. Each thermopile sensor consists of a series-wired array of 100 thermocouples (BiSb/NiCr) deposited on a membrane of Si_3N_4, supported by a surrounding frame of silicon. The three sensors in each array measure the temperature on the bottom and on either side of the glass measurement chamber, leaving the top surface of the chamber unobscured. Each sensor is mounted a distance of 50–100 μm from the outer surface of the glass, allowing the sensor membrane (supporting the thermopile "hot" junctions) to be warmed by heat conducted through the air layer between the sensor and the glass chamber. The rim of the sensor (around which the thermopile cold junctions lie) is adhered to the housing using silver-loaded thermally/electrically conductive epoxy (H20E, Epo-tek, Billerica, MA, USA). The housing immediately behind the sensors is recessed to increase the thermal resistance between it and the membrane, thereby allowing the thermopile hot junctions to follow closely the temperature of the measurement chamber.

The three thermopile sensors in each array are electrically connected in a series using H20E epoxy. The electrical resistance of each of the conductive-epoxy connections is approximately 1 Ω, yielding a sensor with a total resistance of 147 kΩ. The series-connected thermopiles are gold-wire-bonded and silver-soldered to shielded, twisted-pair cables which carry the signals to computer-controlled nanovoltmeters (Agilent 34420A). The voltage signals from up- and downstream thermopile arrays are acquired by the nanovoltmeters, and the instantaneous difference between the two voltage measurements (ΔV) is computed in software. The nanovoltmeters are configured to integrate across an integer number of power line cycles, minimizing the detrimental effects of line-cycle-related interference. Control, data acquisition, and data analysis are provided by software written in National Instrument's LABVIEW 7.1 environment running on a WINDOWSXP computer.

The housing is tightly screwed to the top of a gold-plated brass heat exchanger. After a muscle has been positioned in the center of the measurement chamber, a second heat exchanger can be screwed in place on top of the measurement chamber housing. This configuration allows the possibility of regulating the working temperature of the calorimeter by perfusing the heat exchangers with well-circulated, temperature-controlled water. To date, experiments have been conducted at room temperature.

The entire device is mounted on an optical breadboard beneath a stereo microscope (Stemi SV11, Zeiss, Oberkochen, Germany) and is contained in a thermally insulated, light-proof enclosure.

III. METHODS

During calibration, a custom-built syringe pump (a precision Hamilton syringe driven by a 100:1 geared-down stepper motor) provides a steady flow of superfusate into the calorimeter, controlled to 16.6 nl/s resolution. Throughout the duration of a muscle experiment, the fluid flow is gravity fed, allowing the reservoir of superfusing solution to be vigorously bubbled with oxygen, and minimizing fluid flow rate fluctuations.

To simulate the heat output of a muscle, a sinusoidal current is used to Joule-heat the volume of water between the hooks. A function generator (Agilent 33220A) generates a high-frequency sinusoidal voltage that is externally amplitude modulated by the controlling computer. The heat dissipated by the high-frequency electrical current in the fluid is low-pass filtered by the comparatively slow thermal response of the calorimeter. With tap water flowing through the calorimeter, a carrier wave in the frequency range of 100 kHz-1 MHz was observed to maximize the temperature increase in the fluid. The voltage across, and the current between, the hooks are measured and recorded, allowing the sensitivity of the calorimeter to be readily determined at any given flow rate. The electrical resistance of the water flowing through the bath was observed to remain constant within $\pm 1\%$ throughout the time course of every calibration. This calibration technique can be utilized even while a trabecula is mounted between the hooks. Trabeculae produce no observable or measurable response to the very low amplitude ($\sim$100 mV) and high frequency of this calibration signal.

A detailed finite-element model of the measurement chamber has been generated in the ANSYS/FLOTRAN environment. The model consists of $\sim$200 000 trilinear elements describing the flow of the fluid (assumed to be laminar) and heat (via advection, diffusion, and conduction) in the device. We take advantage of the half symmetry of the microcalorimeter about its centerline in order to reduce the size of the model.

The trabecula is modeled as a heat-generating rectangular prism suspended between the hooks. Viscous heating ef-

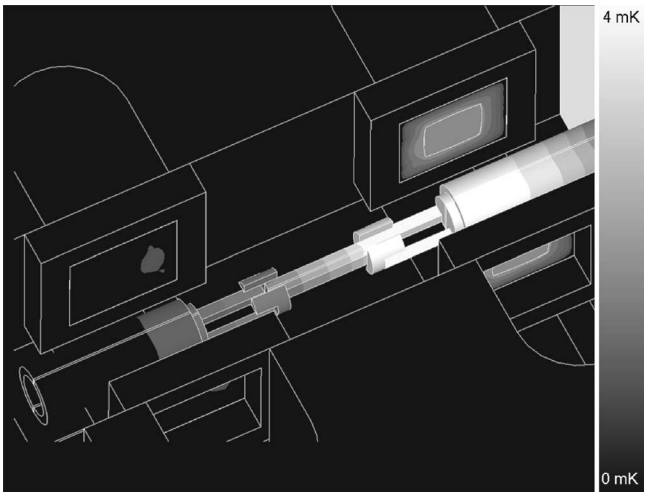

FIG. 2. Steady-state temperature of calorimeter in response to 10 μW heat liberation at a flow rate of 1 μl/s. Fluid flow is from left to right (fluid and measurement chamber not shown).

fects in the fluid are assumed to be negligible.[9] The air surrounding the glass measurement chamber is modeled as a solid conducting medium. Convection currents in the air are ignored.

IV. RESULTS AND DISCUSSION

The finite-element model predicts that the power liberated by a typical trabecula (10 μW) will increase the temperature of the fluid (flowing at 1 μl/s) by approximately 1.6 mK (Fig. 2).

The temperature of the glass measurement chamber (not shown) is maximal slightly downstream of the trabecula and is closely coupled to the temperature of the fluid in the chamber. The temperature of the membrane of the downstream sensor is increased to 85% of the chamber temperature as heat conducts through the thin layer of intervening air. (The chamber and sensor could be more tightly coupled by the use of a thermally conductive paste, or other thermal-coupling method, but this would significantly increase the thermal time constant and the complexity of construction.)

Downstream from the position of the sensor, the temperature of the chamber decreases steadily, indicating significant heat loss through the surrounding air to the thermally massive tellurium-copper housing. A small quantity of heat is also conducted back upstream, primarily through the platinum hook and attached quartz tube, warming the fluid and glass chamber upstream of the heat source.

The tellurium-copper housing of the calorimeter maintains the cold junctions around the rim of the thermopiles at the same constant temperature. Thus, the temperature increase of the fluid can be inferred from the voltage difference between the thermopile signals.

A. Sensitivity

In order to determine the calorimeter's sensitivity (the ratio of temperature difference or voltage difference to dissipated power) the step and steady-state responses of the calorimeter were measured using the following method.

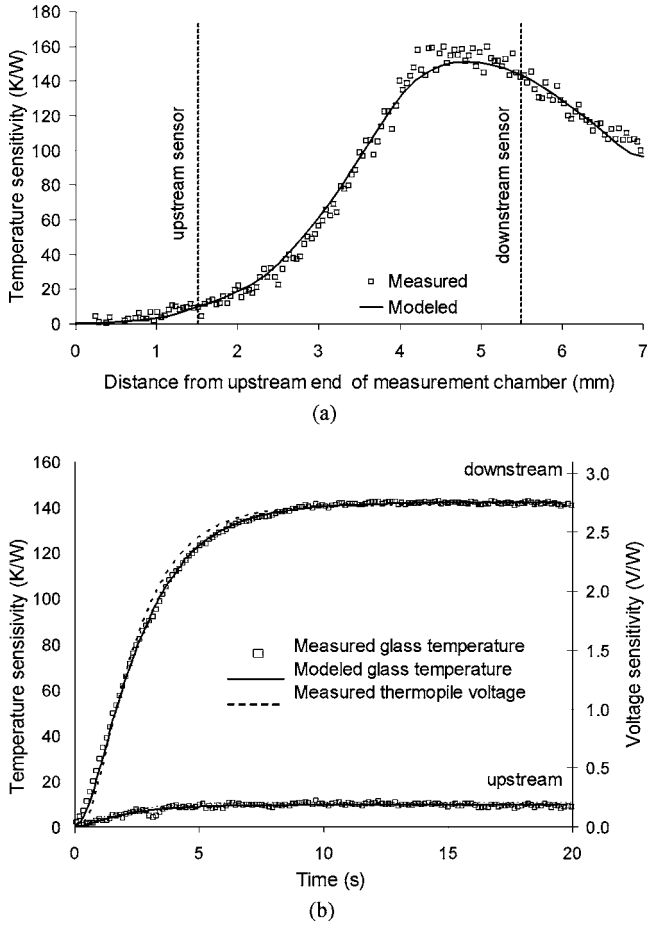

FIG. 3. Measured and modeled calorimeter response. (a) Steady-state temperature distribution along the length of the chamber. (b) Step-response temperature increase at up- and down-stream sensors.

The syringe pump passed tap water through the measurement chamber at a volume flow rate of 1 μl/s. A sinusoidal current (imposed by a 10.0 V_{rms} 50 kHz carrier) was passed between the two platinum hooks, dissipating the power at a rate of about 10 mW. Simultaneously, an infrared-sensitive camera Thermovision A40M Research, with 100 μm closeup lens, FLIR Systems, North Billerica, MA, USA] recorded the temperature distribution on the top surface of the measurement chamber, assuming an infrared emissivity of 0.92 for the chamber's glass surface. The infrared camera, which comprises a 320×240 array of microbolometers, acquires an image with approximately 100 μm/pixel spatial resolution, 80 mK temperature resolution, and 7.5 Hz sampling rate. Two 1 mm^2 areas of interest were defined on the image of the top surface of the measurement chamber adjacent to both up- and downstream sensors, allowing the average temperature change in these positions to be computed. The steady-state temperature profile along the length of the top surface of the chamber was also recorded. Simultaneously, the voltage outputs of up- and down-stream temperature sensors were measured by, and recorded from, the nanovoltmeters. All measurements and model predictions were normalized to an input power of 1 W.

Figure 3(a) compares the measured steady-state (60 s) temperature response along the centerline of the measure-

ment chamber (measured by an infrared camera) with the prediction of the finite-element model.

The measured data confirm the model's prediction of a maximum temperature response of approximately 140 K/W slightly downstream of the heat source. The measured temperature step responses of the calorimeter [Fig. 3(b)] also agree well with the finite-element model predictions. Importantly, the thermopile voltage step responses (dashed lines, right-hand ordinate) closely follow those of the measured chamber temperature, indicating that the conduction time through the intervening air layer is negligible and that the thermopile voltage is closely coupled to the chamber temperature. The ratio of the measured voltage to the modeled thermopile temperature reveals that the thermoelectric sensitivity of the sensors is approximately 23 mV/K. Since each thermopile array consists of 300 thermoelectric junctions, this implies a Seebeck coefficient for each junction of 78 μV/K. The difference between up- and down-stream temperatures shows that the temperature sensitivity of the calorimeter at this flow rate is approximately 130 K/W. That is, for a typical muscle heat output of 10 μW, the difference between up- and downstream temperatures is approximately 1.3 mK.

An important parameter for this calorimeter design is the differential voltage sensitivity (the ratio of the measured voltage difference between the two thermopile sensors to the output of the power source). Over the tested dynamic range of the calorimeter (0–10 mW), the sensitivity (measured at 1 μl/s) remained constant at 2.56±0.05 V/W. This implies that a muscle producing maximal heat output (10 μW) will generate a voltage difference of 25.6 μV.

B. Accuracy, precision, and resolution

The accuracy and precision of the calorimeter were established by the following method: A thick-film resistor (1 KΩ, 0.1 %, Susumu Co. Ltd, RR0816P-102-B-T5) was suspended in the fluid volume between the quartz tubes and wired out through the left tube using 25 μm isonel-insulated platinum wires. By modulating the current through the resistor circuit (100 μA, 33 mHz square wave) the step response of the calorimeter was measured repeatedly. The power (10.0 μW) generated in the resistor provided a known standard to which the calorimeter measurement (calibrated previously using the joule-heating technique) could be compared. At a gravity-driven fluid flow rate of 1.01±0.01 μl/s, the power output measured by the calorimeter (after 15 s) was 10.220±0.014 μW (mean ± standard error, n=76). The majority of the error in the power output measurement may be attributed to the slight changes in the thermal- and fluid-flow pathway caused by the insertion of the thick-film resistor and wiring. Conversely, Joule-heating the fluid between the hooks with a precisely known amount of power allows the sensitivity of the calorimeter to be assessed accurately during an experiment without disturbing the system. The standard error (14 nW) of the mean power provides a measure of the precision of the calorimeter at this flow rate and power range.

The calorimeter's power resolution is fundamentally limited by the noise content of the thermopile voltage signals. The voltage noise has two main origins: temperature fluctuations imposed upon the hot and cold junctions of the thermopile and electrical noise in the thermopile sensor circuit. The thermal noise can be generated by the movement of the air surrounding the chamber, fluctuations in the incoming fluid temperature, and electromagnetic radiation striking the thermopile membrane. Additional low-frequency thermal offsets may also be generated by viscous heating of the fluid as it passes through the chamber.[9] Variations in the flow rate also generate fluctuations in the temperature signal when heat is being liberated in the chamber. The electrical noise is introduced by resistive (Johnson) noise in the thermopile arrays, magnetically and electrically coupled ac voltages, and triboelectric noise arising from the movement of the signal cables. Additional minor electrical offsets can be introduced by thermoelectric junctions formed at connections between dissimilar metals in the wiring.

The thermal noise has been minimized by making the housing and heat exchanger thermally massive, by constructing them from thermally conductive materials (tellurium-copper and brass), and by constraining the volume of air between them and the measurement chamber. The fluid is thermally low-pass filtered by the heat exchanger prior to entering the measurement chamber.

The electrical noise is curtailed by securing the well-shielded twisted-pair cables, and using only copper-copper connections, where possible. The coupled line-cycle noise is reduced by taking advantage of the integrating function of the nanovoltmeters. Increasing the integration time (an integer number of power line cycles) diminishes line-frequency-related noise components. The Johnson noise (ε_R) in the thermopiles (resistance R)

$$\varepsilon_R = \sqrt{4kTR\Delta f} \tag{1}$$

is also reduced as the integration time ($1/\Delta$f) is increased.

To measure the total noise content of the voltage difference signal, the following method was used. Water was passed through the calorimeter at 1 μl/s. With no stimulating current applied, the power spectral density and histogram of the voltage difference were computed across a range of integration times. In each case, the power spectral density function was approximately flat across the measurement bandwidth. A Gaussian function was fitted to the histogram of the ΔV data. Its standard deviation parameter (σ) provides an estimate of the rms noise. Figure 4 shows the rms noise as estimated by this fitting procedure, with the Johnson noise in the thermopiles superimposed for comparison. The right-hand ordinate shows the effective sampling rate corresponding to each integration time.

At longer integration times (corresponding to lower sampling rates) the estimated noise in the thermopiles approaches the theoretical limit set by the Johnson noise in the thermopile tracks. For example, an integration time of 0.33 s (20 power-line cycles) results in a sampling rate of 1.47 Hz, at which the measured RMS noise of 115 nV is comparable with the Johnson noise in the thermocouples (theoretically 120 nV). Consequently, at this flow rate and integration time, the signal-to-noise ratio of the device is approximately

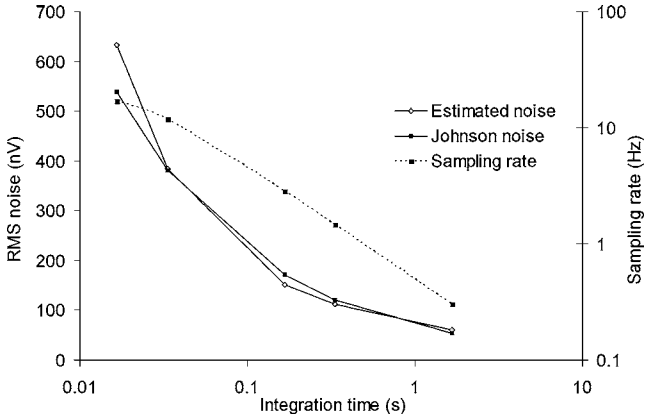

FIG. 4. Noise and sampling rate as a function of integration time.

220:1, and the noise level corresponds to a power output of 45 nW and a temperature change of 5 μK.

For experiments in which the transient response is less important, so that longer integration times can be tolerated, the signal-to-noise ratio can thereby be improved to 500:1 or (with additional digital filtering) higher.

C. Flow-rate dependence

All aforementioned measurements were acquired at a precisely controlled superfusate flow rate of 1 μl/s, a lower limit set by the need to ensure an adequate supply of oxygen to a maximally contracting trabecula of typical dimensions.

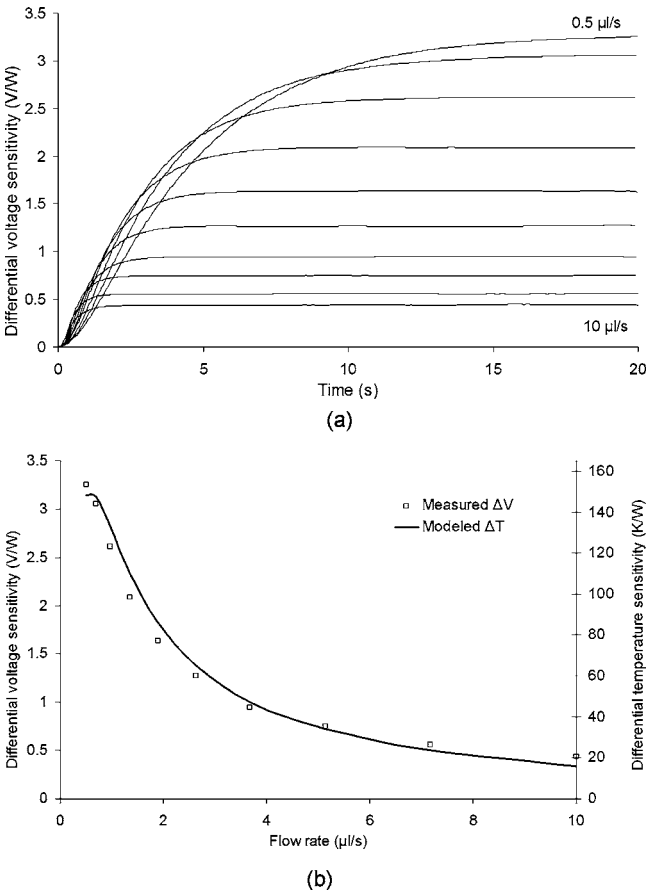

FIG. 5. Calorimeter characteristics as a function of fluid flow rate. (a) Step response. (b) Steady-state sensitivity.

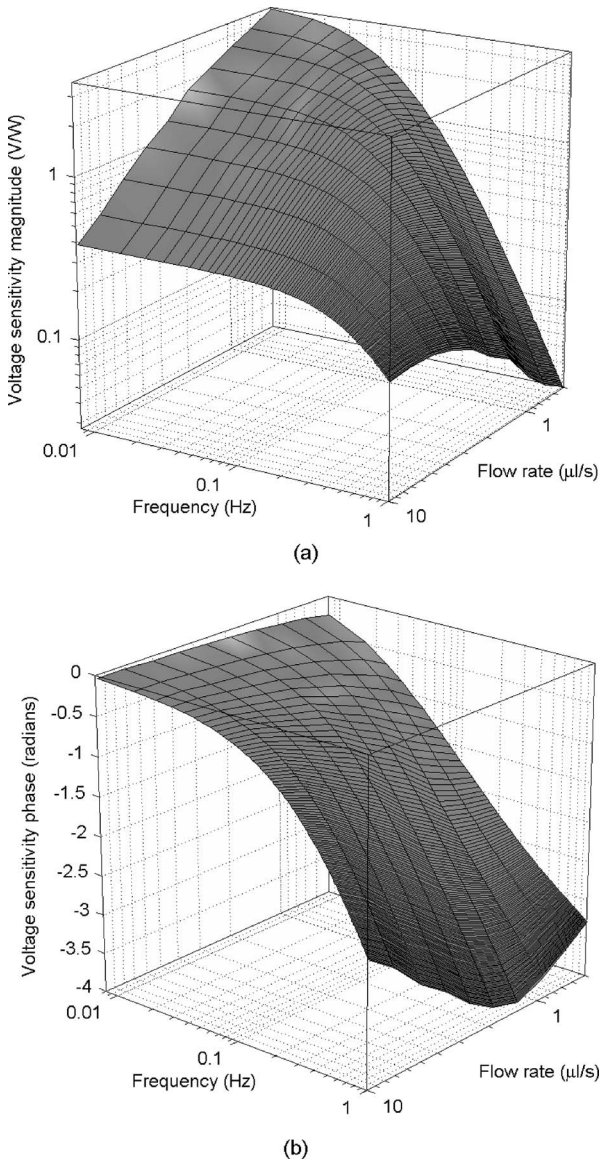

FIG. 6. Calorimeter sensitivity frequency response as a function of fluid flow rate. (a) Magnitude. (b) Phase.

However, syringe-pump-driven flow is not ideal for use during an experiment owing to the high-frequency flow-rate fluctuations that are often generated and the complication of oxygenating the superfusing solution in such a system. During the time course of an experiment, it is preferable to use a gravity-driven flow-through system. The constant superfusate flow rate of a gravity-driven system is readily measured from a collected mass of fluid, but can be difficult to control precisely. Consequently, it is prudent to determine the characteristics of the calorimeter over a range of feasible flow rates.

The response of the calorimeter to step changes of the power output is strongly dependent upon the flow rate [Fig. 5(a)]. The steady-state sensitivity varied between 0.5 and 3.3 V/W over this range of flow rates, while the rise time of the step response varied from less than 1 s at 10 μl/s to approximately 10 s at a flow rate of 0.5 μl/s. Low flow rates allow a greater sensitivity to be achieved, but at the expense of slower responses to high-frequency temperature events.

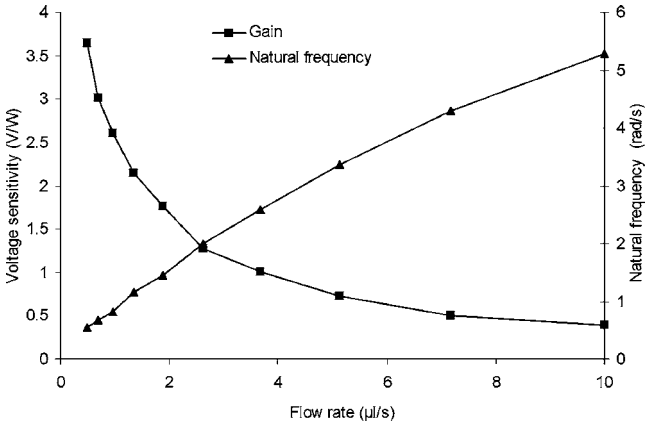

FIG. 7. Fitted gain and natural frequency parameters as functions of fluid flow rate.

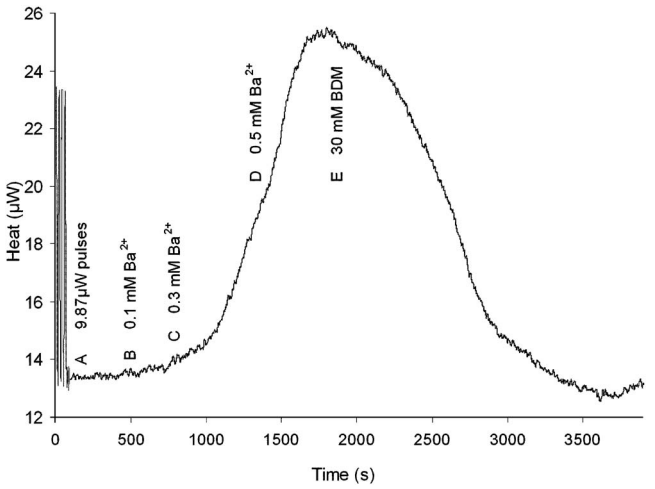

FIG. 8. Heat output of a cardiac trabecula in response to a Ba^{2+} contracture eventually terminated by the introduction of BDM.

The steady-state differential temperature response predicted by the finite-element model [Fig. 5(b), right-hand ordinate] exhibits a similar flow-rate dependency, reducing to a meager 16 K/W at 10 μl/s. As the flow rate approaches zero, conduction begins to dominate advection, such that the developed temperature difference between the up- and downstream sensors decreases.

These characteristics can be more completely interrogated by utilizing linear system identification techniques. By discharging a sequence of pseudorandom binary heat pulses ($\sim$10 V_{rms}, Δt=0.3 s, n=1024) into the fluid between the hooks while acquiring the voltage difference between the two temperature sensors (8192 points, 16.6 Hz sample rate), the frequency response of the voltage response was measured as a function of flow rate. The voltage sensitivity has the characteristic form of an overdamped, second-order, low-pass system with a linear-phase component caused by the time delay between heat injection and response at the downstream sensor. Accordingly, the frequency response of the voltage magnitude was fitted (using an implementation of the Levenberg-Marquardt least-squares algorithm) with the following function:

$$|V(j\omega)| = \left| \frac{S_{ss} \cdot \omega_n^2}{-\omega^2 + 2\zeta\omega_n j\omega + \omega_n^2} \right|, \tag{2}$$

where S_{ss} is the steady-state sensitivity, ω_n is the natural frequency, and ζ is the damping factor. Subsequently, an additional linear-phase component was fitted to the phase data. The fitted magnitude and phase of the voltage frequency-response functions are shown in Fig. 6.

These families of responses allow the user to determine the calorimeter's sensitivity and natural frequency at any realistic flow rate. The steady-state voltage sensitivity (Fig. 7, squares) can be used to relate the measured voltage differences to the power output of the muscle, while the natural frequency (Fig. 7, triangles) defines the effective low-pass cutoff frequency of the calorimeter. Both of these parameters vary by an order of magnitude over the range of flow rates measured, while the fitted damping factor (not shown) is almost independent of flow rate.

Additionally, the sensitivity and step response of the calorimeter may be readily confirmed during an experiment by passing a small high-frequency current between the hooks. A voltage of $\sim$100 mV is sufficient to liberate 10 μW of power in the measurement chamber, and raises the temperature of the fluid by $\sim$1 mK.

D. Verification

Our calorimeter has been designed to measure the energy consumption of cardiac trabeculae under a variety of conditions. Ba^{2+} can be utilized to induce contracture in cardiac muscle, concomitantly increasing the energy expenditure through increasing the degree of crossbridge cycling. To demonstrate the effectiveness of the calorimeter, we performed the following experiment (approved by The University of Auckland Animal Ethics Committee).

A Wistar rat (51 days, 297 g) was killed via stunning and immediate cervical dislocation. The thoracic cavity was opened, and the heart quickly excised and plunged into a dissection solution at 0 ° C to effect arrest. During Langendorff perfusion of the heart with an oxygenated dissection solution,[10] its right ventricle was opened and a trabecula (4 mm long by 400 μm $\times$ 200 μm) excised. The preparation was carefully mounted between the platinum hooks while being continuously superfused with an oxygenated dissection solution containing the negative inotropic agent 2,3-butanedione monoxime (BDM). The hooks were separated until the trabecula was gently but securely held before being carefully introduced into the measurement chamber. Several minutes later, the superfusate was changed to a BDM-free solution, allowing the viability of the muscle to be confirmed by observing its contraction in response to electrical stimulation via the hooks.

After changing the superfusate to a Ca^{2+}-free solution, the sensitivity of the calorimeter was confirmed by passing high-frequency current pulses between the hooks [Fig. 8(A)], as described above.

The subsequent introduction of Ba^{2+} to the superfusate instigated a profound increase in muscle heat production [Figs. 8(B), 8(C), and 8(D), uncertainty of $\pm$45 nW]. With $[Ba^{2+}]$ of 0.5 mM, the heat output of the trabecula reached a peak of approximately 12 μW greater than that observed

prior to contracture. The Ba^{2+} contracture was subsequently reversed [Fig. 8(E)] by the addition a of 40 mM BDM to the solution (which reduced the heat output to a value lower than had been observed prior the to onset of the Ba^{2+} contracture presumably as a consequence 40 mM BDM abolishing all residual actomyosin ATPase activity).[11]

Thus, our microcalorimeter exhibits sufficient sensitivity and has a sufficiently high signal-to-noise ratio, to be useful in detecting the heat output of isolated cardiac trabeculae. It is presently installed and being used in myothermic experiments at the Bioengineering Institute, The University of Auckland, Auckland, New Zealand.

ACKNOWLEDGMENTS

The authors gratefully acknowledge the generous financial support of The New Zealand Foundation for Research, Science, and Technology (Contract No. Mass0101) and the Royal Society of New Zealand (Marsden Fund).

[1] N. P. Smith, C. J. Barclay, and D. S. Loiselle, Prog. Biophys. Mol. Biol. **88**, 1 (2005).
[2] V. J. A. Schouten and H. E. D. J. ter Keurs, Pfluegers Arch. **407**, 1 (1986).
[3] J. Daut and G. Elzinga, J. Physiol. (London) **398**, 1 (1988).
[4] J. Daut and G. Elzinga, J. Physiol. (London) **413**, 1 (1989).
[5] D. Köhnke, M. Schramm, and J. Daut, Mol. Cell. Biochem. **174**, 1 (1997).
[6] M. Zieren, and J. M. Köhler, Fresenius' J. Anal. Chem. **358**, 6 (1997).
[7] K. Verhaegen, K. Baert, J. Simaels, and W. Van Driessche, Sens. Actuators, A **82**, 1 (2000).
[8] B. Xie, M. Mecklenburg, B. Danielsson, O. Öhman, and F. Winquist, Anal. Chim. Acta **299**, 165 (1994).
[9] D. S. Loiselle., G. J. M. Stienen, C. van Hardeveld, E. T. van der Meulen, G. I. Zahalak, J. Daut, and G. Elzinga, J. Gen. Physiol. **108**, 6 (1996).
[10] R. S. Kirton, A. J. Taberner, P. M. F. Nielsen, A. A. Young, and D. S. Loiselle, Exp. Physiol. **89**, 5 (2004).
[11] R. S. Kirton, A. J. Taberner, P. M. F. Nielsen, A. A. Young, and D. S. Loiselle, Am. J. Physiol. Heart Circ. Physiol. **288**, 4 (2005).